Title

Adrenergic pathway activation enhances brown adipose tissue metabolism: A [18F]FDG PET/CT study in mice

Journal

Nuclear Medicine and Biology, 41(1)

ISSN

0969-8051

Authors

Mirbolooki, M Reza
Upadhyay, Sanjeev Kumar
Constantinescu, Cristian C
et al.

Publication Date

2014

DOI

10.1016/j.nucmedbio.2013.08.009

Peer reviewed

Published in final edited form as:
Nucl Med Biol. 2014 January ; 41(1): . doi:10.1016/j.nucmedbio.2013.08.009.

Adrenergic pathway activation enhances brown adipose tissue metabolism: A [^{18}F]FDG PET/CT study in mice

M. Reza Mirbolooki[a], **Sanjeev Kumar Upadhyay**[b], **Cristian C. Constantinescu**[a], **Min-Liang Pan**[a], and **Jogeshwar Mukherjee**[a,b]

[a]Preclinical Imaging, Department of Radiological Sciences, School of Medicine, University of California, Irvine

[b]Department of Physiology and Biophysics, School of Medicine, University of California, Irvine

Abstract

Objective—Pharmacologic approaches to study brown adipocyte activation *in vivo* with a potential of being translational to humans are desired. The aim of this study was to examine pre- and postsynaptic targeting of adrenergic system for enhancing brown adipose tissue (BAT) metabolism quantifiable by [^{18}F]fluoro-2-deoxyglucose ([^{18}F]FDG) positron emission tomography (PET)/ computed tomography (CT) in mice.

Methods—A β_3-adrenoreceptor selective agonist (CL 316243), an adenylyl cyclase enzyme activator (forskolin) and a potent blocker of presynaptic norepinephrine transporter (atomoxetine) were injected through the tail vein of Swiss Webster mice 30 minutes before intravenous (iv) administration of [^{18}F]FDG. The mice were placed on the PET/CT bed for 30 min PET acquisition followed by 10 min CT acquisition for attenuation correction and anatomical delineation of PET images.

Results—Activated interscapular (IBAT), cervical, periaortic and intercostal BAT were observed in 3-dimentional analysis of [^{18}F]FDG PET images. CL 316243 increased the total [^{18}F]FDG standard uptake value (SUV) of IBAT 5-fold greater compared to that in placebo-treated mice. It also increased the [^{18}F]FDG SUV of white adipose tissue (2.4-fold), and muscle (2.7-fold), as compared to the control. There was no significant difference in heart, brain, spleen and liver uptakes between groups. Forskolin increased [^{18}F]FDG SUV of IBAT 1.9-fold greater than that in placebo-treated mice. It also increased the [^{18}F]FDG SUV of white adipose tissue (2.2-fold) and heart (5.4-fold) compared to control. There was no significant difference in muscle, brain, spleen, and liver uptakes between groups. Atomoxetine increased [^{18}F]FDG SUV of IBAT 1.7-fold greater than that in placebo-treated mice. There were no significant differences in all other organs compared to placebo-treated mice except liver (1.6 fold increase). A positive correlation between SUV levels of IBAT and CT hounsfiled unit (HU) (R^2=0.55, $p<0.001$) and between CT HU levels of IBAT and liver (R^2=0.69, $p<0.006$) was observed.

Conclusions—The three pharmacologic approaches reported here enhanced BAT metabolism by targeting different sites in adrenergic system as measured by [^{18}F]FDG PET/CT.

Address Correspondence to: Jogesh Mukherjee, PhD, Preclinical Imaging, Department of Radiological Sciences, Medical Sciences B-138, University of California, Irvine, Irvine, CA 92697-5000, Tel: 949-824-2018, Fax: 949-824-2344, j.mukherjee@uci.edu.

Keywords

Brown fat; molecular imaging; diabetes; obesity; BAT

1. INTRODUCTION

Brown adipose tissue (BAT) is well known as a major glucose disposal tissue [1]. BAT is innervated by norepinephrine containing neuronal fibers [2], which interact with β_3-adrenoreceptor (β_3-AR) resulting in the enhancement of glycolysis. This results most likely in an increase in the synthesis of cyclic AMP (cAMP) (Fig. 1) and the consequent overexpression of uncoupling protein-1, UCP1 [3]. Targeting post-synaptic β_3-AR on brown adipocytes has been the most commonly evaluated strategy for studying BAT biology and activating it as a therapeutic approach for diabetes and obesity. However, studies on presynaptic proteins (e.g. norepinephrine transporter, NET) or at the level of secondary messenger (e.g. adenylyl cyclase) are limited and less understood.

Thus, our goal in this study was to investigate three aspects (Fig-1) of adrenergic pathway activation (presynapse to postsynapse to second messenger) on [^{18}F]FDG uptake in BAT of mice using whole-body PET/CT scans. This included increasing presynaptic norepinephrine by blocking NET using atomoxetine, activation of post-synaptic 3 receptors by agonist CL 316243 and increasing cAMP by activation of adenylyl cyclase using forskolin (Fig-1). Atomoxetine is a potent and highly selective blocker (K_i=5×10^{-9} M) of presynaptic NET that is used for treatment of attention-deficit/hyperactivity disorder (ADHD) [4]. Atomoxetine leads to increased synapse concentrations of norepinephrine and therefore an increase in adrenergic neurotransmission [5]. Uptake of a highly selective NET ligand, ^{11}C-MRB ((S,S)-O-[^{11}C]methylreboxetine), suggests the existence of these transporters in BAT [6]. We have recently reported atomoxetine effects on BAT metabolism that are visible and quantifiable by [^{18}F]FDG PET in rats [7]. Binding affinity of CL 316243 for postsynaptic β-adrenergic receptors are Ki: $\beta_1 \geq 10^{-4}$ M; β_2=3×10^{-5} M; β_3=3×10^{-9} M. Chronic CL 316243 administration has been shown to have an antiobesity effect in mice [10]. We have previously reported quantitative assessment of CL 316243-mediated activation of BAT in rats using [^{18}F]FDG PET [11]. Forskolin activates the adenylyl cyclase enzyme directly and increases the intracellular levels of cAMP with a Kd=14.8×10^{-9}M [8]. Forskolin is known as an inducer of thermogenic response in BAT [9].

[^{18}F]FDG PET is the most commonly used modality to assess BAT in humans [12]. Despite the well-established literature of BAT biology in animal models, quantitative analysis of [^{18}F]FDG PET/CT images in mice is now emerging [13]. Mice were optimal for studies reported here since they were small compared with the axial field of view of both Inveon PET (12.7 cm) and MM CT with large area detector (10 cm), which allowed for whole-body imaging in a single session and bed position, compared to our previous rat study where whole body imaging in a single scan was not possible [7,11].

Our specific objectives in this study were: 1. Evaluate the magnitude of BAT activity caused by acute drug treatments of atomoxetine, CL 316243, and forskolin; 2. Examine whether the magnitude of BAT activity was correlated with [^{18}F]FDG uptake in other organs/tissues (e.g. white adipose tissue, skeletal muscle, heart, brain, liver, and spleen). 3. Since CT has also been reported to show changes in activated BAT likely due to lipolysis [14], we examined whether quantitative CT, as a measure of lipid consumption, could identify the same anatomic locations of BAT as [^{18}F]FDG PET and whether CT hounsfield units (HU) are correlated with [^{18}F]FDG PET standard uptake values (SUV) in BAT.

2. MATERIALS AND METHODS

2.1. Animals

Male Swiss Webster mice, aged 14-18 weeks were used in this study. Mice were purchased from Harlan Laboratories (Placentia, CA) and housed under controlled temperatures of 22°C ± 1°C, in a 12-h light–dark cycle, on at 6:00 AM, with water and food chow ad libitum. All animal studies were approved by the Institutional Animal Health Care and Use Committee of University of California, Irvine.

2.2. Equipment

An Inveon dedicated PET scanner (Siemens Medical Solutions, Knoxville, TN), which has a resolution of 1.46 mm in the center of the field-of-view, was used for the PET studies. An Inveon Multimodality (MM) CT scanner (Siemens Medical Solutions, Knoxville, TN) was used for CT acquisitions in combined PET/CT experiments. A Sigma Delta anesthetic vaporizer (DRE, Louisville, KY) was used to induce and maintain anesthesia during intravascular injections and PET/CT acquisitions.

2.3. Chemicals

Atomoxetine and forskolin were purchased from Sigma-Aldrich (St. Louis, MO). CL 316243 was purchased from Tocris Bioscience (Bristol, United Kingdom). [^{18}F]FDG was obtained from PETNET solutions (Irvine, CA). Isoflurane was purchased from Clipper Distributing Company (St. Joseph, MO).

2.4. Experimental protocol

All mice (n=12) were fasted for at least 17 hours before [^{18}F]FDG administration. They were randomly divided into four groups. For targeting presynaptic NET, mice (n=3, Wt: 37.0±6.6 g) were injected with atomoxetine (1mg/kg, IV 0.02 mL); for targeting adenylyl cyclase, mice (n=3, Wt: 36.3±6.6 g) were injected with forskolin (1mg/kg, IV 0.02 mL); for targeting post-synaptic β_3-AR, mice (n=3, Wt: 40±5.5 g) were injected with CL 316243 (1mg/kg, IV 0.02 mL); and placebo-treated mice (n=3, Wt: 40±5.5 g) were injected IV with normal saline (0.02 mL) through the tail vein 30 minutes before IV administration of [^{18}F]FDG under 2% isoflurane anesthesia (Fig. 2). Mice were awake between the injections and free to move in their cages. They were eventually placed in the supine position in a mouse holder and anesthetized with 2% isoflurane for whole-body PET imaging. The mouse holder was placed on the PET/CT bed and 30 minute-long PET scans were acquired 60 minutes after [^{18}F]FDG injections. All animals had a 10-minute-long CT scan after the PET scan for attenuation correction and anatomical delineation of PET images. The same method of injection of [^{18}F]FDG was used for all mice, as was the recovery period and re-anesthetization for PET.

It should be noted that the drugs and [^{18}F]FDG was injected intravenously in less than 3 minutes under anesthesia while they were placed on a warm pad. The animals were then allowed to recover immediately (less than a minute) and uptake of [^{18}F]FDG occurred for one hour while the animals were awake. Thus the effect of anesthesia was minimized and was used for the PET/CT scan after the [^{18}F]FDG uptake had occurred.

2.5. PET/CT imaging

The Inveon PET and MM CT scanners were placed in the “docked mode” for combined PET/CT experiments. PET data were reconstructed as 128 × 128 × 159 matrices with a transaxial pixel of 0.776 mm and slice thickness of 0.796 mm using an OSEM2D algorithm (16 subsets, 4 iterations, 2 EM iterations). PET images were corrected for random

coincidences, attenuation and scatter. All images were calibrated in units of Bq/cm^3 by scanning a Ge-68 cylinder (6 cm diameter) with known activity and reconstructing the acquired image with parameters identical to those of [^{18}F]FDG images. The CT images were spatially transformed to match the reconstructed PET images. The CT projections were acquired with the detector-source assembly rotating over 360 degrees and 720 rotation steps. A projection bin factor of 4 was used in order to increase the signal to noise ratio in the images. The CT images were reconstructed using cone-beam reconstruction with a Shepp filter with cutoff at Nyquist frequency and a binning factor of 2 resulting in an image matrix of 480 × 480 × 632 and a voxel size of 0.206 mm.

2.6. Image analysis

The magnitude of BAT [^{18}F]FDG activation was expressed as SUV which was computed as the average [^{18}F]FDG activity in each volume of interest, VOI (in kBq/mL) divided by the injected dose (in MBq) times the body weight of each animal (in Kg). For quantitative analysis, VOIs were drawn on PET images for interscapular BAT (IBAT), and heart myocardium. Similarly to previously described methods, [7] the VOIs were delineated visually by auto-contouring the [^{18}F]FDG activity that was clearly above normal background activity in mice treated with drugs. The VOIs were delineated visually on CT images for interscapular white adipose tissue (IWAT), skeletal muscle (Triceps Brachii), brain, spleen, and liver. All in vivo images were analyzed using PMOD Software (PMOD Technologies, Zurich, Switzerland) and Inveon Research Workplace (IRW) software (Siemens Medical Solutions, Knoxville, TN).

2.7. Photomicrograph production

All original in vivo images were processed with either PMOD Software (PMOD Technologies, Zurich, Switzerland) or Inveon Research Workplace (IRW) software (Siemens Medical Solutions, Malvern, PA). Image captures of the originals were then inserted and sorted in Microsoft PowerPoint 2010 to produce final images, which then were saved as .TIFF files. No modifications to contrast or brightness were done.

2.8. Statistical analysis

Statistical differences between groups were determined using one way ANOVA followed by post hoc Fisher's Least Significant Difference (LSD) test in IBM SPSS, version 20 for Windows (Armonk, NY). Levene's test was used to examine the homogeneity of variances. If the variances were not equal, a variance-stabilizing transformation was chosen [$f\,x = \mathrm{Ln}\,x$] to allow the application of one way ANOVA. We calculated the statistical power with two-sample test based on IBAT SUV data obtained from CL 316243 experiments, which was equal to 1.0. Using bivariate analysis, scatter plots were created for the computation of square of correlation coefficients (R^2) between different variables. A p value of <0.05 was considered to indicate statistical significance.

3. RESULTS

3.1. Drug-induced activated BAT

Treatment of mice with 1 mg/kg of each of the three studied drugs at ambient temperature increased the total [^{18}F]FDG uptake of all regions of BAT. Activated interscapular, cervical, periaortic and intercostal BATs were observed in 3-dimentional analysis of [^{18}F]FDG PET images and regions were confirmed anatomically by CT co-registration (Fig-3A). This regional distribution was consistent among different mice treated with the drugs. In control mice, the rank of [^{18}F]FDG uptake was similar, but with lower intensities. Smaller areas such as the intercostal BAT were difficult to discern under control conditions. We chose to

compare IBAT uptake between the groups due to its more consistent shape, as described previously [11]. Figure-3B shows ventral, lateral, and dorsal views of IBAT in mice treated with CL 316243. CT HU changes were visible only when BAT was highly active, but it did not assist in differentiating BAT from the surrounding tissues (Fig-4).

3.2. Effect of CL 316243 on [^{18}F]FDG SUV and CT HU in BAT

PET images revealed high [^{18}F]FDG uptake in IBAT of CL 316243 treated mice at ambient temperature (Fig-5A and B). The effect of increased [^{18}F]FDG was consistent across animals treated with CL 316243. It increased the total [^{18}F]FDG SUV of IBAT to 4.3±2.2 which is 5.0-fold greater ($p<0.001$) compared to [^{18}F]FDG SUV in placebo-treated mice of 0.86±0.09. CL 316243 also increased the [^{18}F]FDG SUV of IWAT (2.4-fold) and muscle (2.7-fold) as compared to the control. However, the increased values in IWAT and muscle due to CL 316243 were below BAT values of placebo-treated mice. Heart [^{18}F]FDG uptake increased and brain [^{18}F]FDG uptake decreased but changes were not statistically significant. There was no significant difference in spleen and liver uptakes between groups. The SUV data in all regions are summarized in Table 1. CT images revealed that CL 316243 increased CT HU of IBAT to −129±87 which is 1.1-fold greater than the CT HU in placebo-treated mice of −144±90, but the difference was not statistically significant (Fig. 5A and B). There was no significant difference in IWAT CT HU between CL 316243-treated and control groups (-302±69 vs. −239±148).

3.3. Effect of forskolin on [^{18}F]FDG SUV and CT Hounsfield unit in BAT

PET images revealed mild [^{18}F]FDG uptake in IBAT of forskolin treated mice at ambient temperature (Fig-5A and B). Forskolin increased [^{18}F]FDG SUV of IBAT to 1.64±0.47 which is 1.9-fold greater ($p<0.05$) than that of [^{18}F]FDG SUV in placebo-treated mice of 0.86±0.09. Forskolin also increased the [^{18}F]FDG SUV of IWAT (2.2-fold) compared to control. However, the increased values were below the level of BAT values in non-treated mice. Heart [^{18}F]FDG uptake increased significantly at a level higher than that of IBAT in the same mice (5.4-fold). There was no significant difference in muscle, brain, spleen and liver uptakes between groups. The SUV data in all regions are summarized in Table 1. CT images revealed that forskolin increased CT HU of IBAT to −97±9 which is 1.5-fold greater compared to CT HU in placebo-treated mice of −144±90, but the difference was not statistically significant (Fig. 5A and B). Forskolin also increased CT HU of IWAT to −185±16 which is 1.3-fold greater compared to CT HU in placebo-treated mice of −239±148, but the difference was not statistically significant.

3.4. Effect of atomoxetine on [^{18}F]FDG SUV and CT Hounsfield unit in BAT

PET images revealed mild [^{18}F]FDG uptake in IBAT of ATX treated mice at ambient temperature (Fig-5A and B). ATX increased [^{18}F]FDG SUV of IBAT to 1.52±0.35 which is 1.7-fold greater ($p<0.05$) than that in placebo-treated mice of 0.86±0.09. There was no significant difference in all other organ uptakes compared to placebo-treated mice except in liver. ATX increased the [^{18}F]FDG SUV of liver (1.6-fold) as compared to control. The SUV data in all regions are summarized in Table 1. CT images revealed no significant changes in CT HU of IBAT and IWAT of treated mice compared to those of placebo-treated mice (Fig-5A and B).

3.5. Correlations between BAT [^{18}F]FDG SUV and other organs [^{18}F]FDG SUV and CT HU

Regardless of the method of activation, close positive correlations between IBAT and IWAT SUV levels ($y=0.2311x+0.2532$, $R^2=0.49$, $p<0.02$; Fig-6A) and of IBAT and muscle ($y=0.1601x+0.0425$, $R^2=0.66$, $p<0.001$, Fig-6B) were observed. A negative correlation between SUV levels of IBAT and brain ($y=-0.6121x+3.167$, $R^2=0.54$, $p<0.01$) was observed

(Fig-6D). There were no significant correlations between SUV levels of IBAT and those of heart myocardium, liver and spleen (Fig-6C,E,F). A close positive correlation between SUV levels of IBAT and CT HU ($y=25.059\times-185.5$, $R^2=0.55$, $p<0.001$) was observed (Fig-7). No significant correlation was found between SUV and HU in IWAT. Interestingly, a very close positive correlation between CT HU levels of IBAT and liver ($y=0.3311x-14.741$, $R^2=0.69$, $p<0.006$) was observed (Fig-8). There were no significant correlations between IBAT CT HU and other organs.

4. DISCUSSION

All three studied drugs, CL 316243, atomoxetine and forskolin, were able to activate BAT and measured with [^{18}F]FDG PET imaging in mice. Because of the high affinity and selective nature of CL 316243, the increase in BAT [^{18}F]FDG SUV was 5-fold as compared to control mice. This is consistent with our recently reported activated BAT in rats with CL 316243 treatment which was 7-fold more than controls [11]. Atomoxetine increased BAT [^{18}F]FDG SUV 1.5-fold as compared to control mice and is similar to our recent report of activated BAT in rats with atomexetine [7]. Forskolin directly activates adenylyl cyclase and raises cAMP levels in a wide variety of cell types [16]. Forskolin increased BAT [^{18}F]FDG SUV 1.6-fold as compared to control mice. Correlation of IBAT activation by the three drugs in IWAT, muscle and brain were stronger, compared to heart, liver and spleen (Fig-6). These findings suggest that activation of BAT is being mediated by the second messenger cAMP. However, other mechanisms of BAT activation cannot be ruled out. Currently, the prevalence of inactive BAT in the adult population is reportedly low [17-19], which dampens its potential significance for altering adult human metabolism. BAT is only active when its thermogenic function is required [20] and [^{18}F]FDG uptake is a direct consequence of tissue activity [3], therefore, inactive brown adipose tissue would not be visible on PET scans. Exposure to cold temperature prior to PET is the only current method to study BAT in humans, a function also mediated by the β-adrenergic system [12]. Large variations in sympathetic responses to low temperature [17] limits the use of cold for BAT activation. Pharmacologic approaches such as reported here could be used to study BAT and brown adipocytes biology in different transgenic mice models and humans.

We observed significant [^{18}F]FDG SUV increase in IWAT with both CL 316243 (2.4-fold) and forskolin (2.2-fold) treatment, but not with atomextine as compared to control mice. High levels of β_3-adrenoceptor mRNA have been found in white adipose tissues [21]. Rodent white adipocytes exhibit a strong response to β_3-adrenoreceptor agonists through cAMP production [22]. Five adrenoceptor subtypes are involved in the adrenergic regulation of white adipocytes function. The balance between the various adrenoceptor subtypes is the point of regulation that determines the final effect of different drugs on adipocytes [23]. The effects on cAMP production and cAMP-related cellular responses are mediated through the control of adenylyl cyclase activity by the stimulatory β_1-, β_2-, and β_3-adrenoreceptors and the inhibitory α_2-adrenoceptors. The affinity of the β_3-adrenoceptor for norepinephrine is less than that of the β_1- and β_2-adrenoceptors. Conversely, norepinephrine has a higher affinity for the α_2-adrenoceptors than for β_1-, β_2-, or β_3-adrenoceptors. In the presence of atomoxetine, accumulated norepinephrine in synapse likely activates α_2-adrenoceptors more than β_3-adrenoceptors resulting in IWAT inactivation. This effect is absent in BAT likely because α_2-adrenoceptors that are present on rodent white adipocytes are absent in brown adipocytes [24].

A significant [^{18}F]FDG SUV increase in skeletal muscle with CL 316243 (2.7-fold) was observed, but not with forskolin and atomoxetine treatments when compared to control mice. Most functional and receptor binding studies indicate that the β_2-adrenoceptor is the predominant β-adrenoceptor subtype in skeletal muscle [25]. There is increasing evidence

for the presence of a β3-adrenoceptor in skeletal muscle. A range of selective β_3-adrenoceptor compounds have been found to be potent and selective stimulants of non-shivering thermogenesis [26] in rat skeletal muscle. However, β_3-adrenoceptor agonists do not stimulate cAMP accumulation in rat skeletal muscle suggesting that the previously reported increase in glucose uptake by β_3-adrenoceptor agonists in skeletal muscle does not involve direct stimulation of adenylyl cyclase [27]. Therefore, the absence of effect in forskolin and atomoxetine treated groups is likely due to lack of adenylyl cyclase and low affinity of norepinephrine to β_3-adrenoceptors, respectively.

In our study, the CT HUs of BAT were greater under activated conditions by CL 316243 and forskolin, but the differences were not statistically significant. The difference was visible (Fig-7), however it did not assist in localizing BAT as increased CT HUs made IBAT indistinguishable from surrounding muscle due to the loss of contrast. Changes in CT HUs under activated conditions for BAT has been reported previously [14]. Upon activation by adrenergic input, BAT increases its energy demand and burns both glucose and lipids to produce heat [28]. Consumption of stored lipid may be the predominant cause of the increase in CT HUs with BAT activation [14]. A positive correlation between SUV levels and CT HUs of IBAT at higher SUV levels suggests that rise in CT HUs is likely due to lipid consumption in BAT as a consequence of insufficient glucose. A positive correlation was also observed between CT HU levels of IBAT and liver. Chronic administration of β_3-adrenoceptor agonists decrease adiponectin receptor 2 expression in the liver of *db*/*db* mice as a result of the induced amelioration of lipid metabolism [29]. The presence of BAT in adult human has been reported to be independently associated with a lower likelihood of non-alcoholic fatty liver disease diagnosed by CT findings [30]. Adrenergic activation of BAT might have the potential to be a novel therapeutic approach to fatty liver disease.

Specific mRNA for β_3-adrenoreceptor is present in human BAT [31], however, CL 316243 has only a 10-fold selectivity for human β_3- over β_2-adrenoceptors [32]. Moreover, β_3-adrenoceptor mRNA is expressed in the human heart [15] ,which increases the concerns regarding its cardiovascular side effects. CL 316243 has been reported not affect heart rate, systolic and/or diastolic blood pressures, ECG intervals and does not develop tremors [33]. However, physiological role of the corresponding β_3-adrenoreceptor on human myocardium is yet to be completely understood [15]. On the other hand, forskolin increased heart myocardium [^{18}F]FDG and side effects of forskolin include headaches, decreased blood pressure and a rapid heart rate. It has inotropic and vasodilatory properties both in vitro and in vivo and changes in contractility parallel an increase in cAMP concentration and calcium transport into the myocardium [34]. Once the cardiovascular side effects of β_3-adrenoceptor agonists are fully understood, newer drugs targeting this receptor may therefore have a potential for the treatment of type 2 diabetes [35].

CONCLUSIONS

The ability to visualize and quantify BAT glucose and lipid metabolism in mice on whole body [^{18}F]FDG PET/CT imaging has significant implications. All three pharmacologic approaches reported here could enhance BAT metabolism by targeting adrenergic system and [^{18}F]FDG PET/CT were able to quantify the magnitude of metabolism. This non-invasive in vivo imaging enables us to study the BAT metabolism and assists in understanding the behavior of other organs under different treatment conditions. BAT activity is correlated with [^{18}F]FDG uptake in other organs such as white adipose tissue, and skeletal muscle. The IBAT CT HU change, as a marker of lipid consumption, was able to confirm the anatomic location of IBAT using [^{18}F]FDG PET; and was positively correlated with that of liver.

Acknowledgments

The authors would like to thank Syed Abbas Naqvi and Nina Thorosian for their technical assistance. The project described was supported by the National Institute of Diabetes and Digestive and Kidney Diseases (NIDDK) with award numbers RC1DK087352 and R21DK092917.

REFERENCES

[1]. Nedergaard J, Bengtsson T, Cannon B. New powers of brown fat: fighting the metabolic syndrome. Cell Metab. 2011; 13(3):238–40. [PubMed: 21356513]

[2]. De Matteis R, Ricquier D, Cinti S. TH-, NPY-, SP-, and CGRP-immunoreactive nerves in interscapular brown adipose tissue of adult rats acclimated at different temperatures: an immunohistochemical study. J Neurocytol. 1998; 27(12):877–86. [PubMed: 10659680]

[3]. Inokuma K, Ogura-Okamatsu Y, Toda C, Kimura K, Yamashita H, Saito M. Uncoupling protein 1 is necessary for norepinephrine-induced glucose utilization in brown adipose tissue. Diabetes. 2005; 54(5):1385–91. [PubMed: 15855324]

[4]. Garnock-Jones KP, Keating GM. Atomoxetine: a review of its use in attention-deficit hyperactivity disorder in children and adolescents. Paediatr Drugs. 2009; 11(3):203–26. [PubMed: 19445548]

[5]. Bymaster FP, Katner JS, Nelson DL, Hemrick-Luecke SK, Threlkeld PG, Heiligenstein JH, Morin SM, Gehlert DR, Perry KW. Atomoxetine increases extracellular levels of norepinephrine and dopamine in prefrontal cortex of rat: a potential mechanism for efficacy in attention deficit/hyperactivity disorder. Neuropsychopharmacology. 2002; 27(5):699–711. [PubMed: 12431845]

[6]. Lin SF, Fan X, Yeckel CW, Weinzimmer D, Mulnix T, Gallezot JD, Carson RE, Sherwin RS, Ding YS. Ex Vivo and In Vivo Evaluation of the Norepinephrine Transporter Ligand [(11)C]MRB for Brown Adipose Tissue Imaging. Nucl Med Biol. 2012

[7]. Mirbolooki MR, Constantinescu CC, Pan ML, Mukherjee J. Targeting presynaptic norepinephrine transporter in brown adipose tissue: A novel imaging approach and potential treatment for diabetes and obesity. Synapse. 2013; 67(2):79–93. [PubMed: 23080264]

[8]. de Jesus LA, Carvalho SD, Ribeiro MO, Schneider M, Kim SW, Harney JW, Larsen PR, Bianco AC. The type 2 iodothyronine deiodinase is essential for adaptive thermogenesis in brown adipose tissue. J Clin Invest. 2001; 108(9):1379–85. [PubMed: 11696583]

[9]. Kitao N, Hashimoto M. Increased thermogenic capacity of brown adipose tissue under low temperature and its contribution to arousal from hibernation in Syrian hamsters. Am J Physiol Regul Integr Comp Physiol. 2012; 302(1):R118–25. [PubMed: 21993529]

[10]. Yoshida T, Sakane N, Wakabayashi Y, Umekawa T, Kondo M. Anti-obesity and anti-diabetic effects of CL 316,243, a highly specific beta 3-adrenoceptor agonist, in yellow KK mice. Life Sci. 1994; 54(7):491–8. [PubMed: 8309351]

[11]. Mirbolooki MR, Constantinescu CC, Pan ML, Mukherjee J. Quantitative assessment of brown adipose tissue metabolic activity and volume using [18F]FDG PET/CT and β3-adrenergic receptor activation. EJNMMI Res. 2011; 1(1):30. [PubMed: 22214183]

[12]. van Marken Lichtenbelt WD, Vanhommerig JW, Smulders NM, Drossaerts JM, Kemerink GJ, Bouvy ND, Schrauwen P, Teule GJ. Cold-activated brown adipose tissue in healthy men. N Engl J Med. 2009; 360(15):1500–8. [PubMed: 19357405]

[13]. Wang X, Minze LJ, Shi ZZ. Functional imaging of brown fat in mice with [18F]FDG micro-PET/CT. J Vis Exp. 2012; (69)

[14]. Baba S, Jacene HA, Engles JM, Honda H, Wahl RL. CT Hounsfield units of brown adipose tissue increase with activation: preclinical and clinical studies. J Nucl Med. 2010; 51(2):246–50. [PubMed: 20124047]

[15]. Michel MC, Harding SE, Bond RA. Are there functional beta(3)-adrenoceptors in the human heart? Br J Pharmacol. 2011; 162(4):817–22. [PubMed: 20735409]

[16]. Insel PA, Ostrom RS. Forskolin as a tool for examining adenylyl cyclase expression, regulation, and G protein signaling. Cell Mol Neurobiol. 2003; 23(3):305–14. [PubMed: 12825829]

[17]. Au-Yong IT, Thorn N, Ganatra R, Perkins AC, Symonds ME. Brown adipose tissue and seasonal variation in humans. Diabetes. 2009; 58(11):2583–7. [PubMed: 19696186]

[18]. Cypess AM, Lehman S, Williams G, Tal I, Rodman D, Goldfine AB, Kuo FC, Palmer EL, Tseng YH, Doria A, Kolodny GM, Kahn CR. Identification and importance of brown adipose tissue in adult humans. N Engl J Med. 2009; 360(15):1509–17. [PubMed: 19357406]

[19]. Stefan N, Pfannenberg C, Haring HU. The importance of brown adipose tissue. N Engl J Med. 2009; 361(4):416–7. author reply 8-21. [PubMed: 19630141]

[20]. Cannon B, Nedergaard J. Brown adipose tissue: function and physiological significance. Physiol Rev. 2004; 84(1):277–359. [PubMed: 14715917]

[21]. Granneman JG, Lahners KN. Differential adrenergic regulation of beta 1- and beta 3-adrenoreceptor messenger ribonucleic acids in adipose tissues. Endocrinology. 1992; 130(1): 109–14. [PubMed: 1309320]

[22]. Langin D, Tavernier G, Lafontan M. Regulation of beta 3-adrenoceptor expression in white fat cells. Fundam Clin Pharmacol. 1995; 9(2):97–106. [PubMed: 7628838]

[23]. Lafontan M, Berlan M. Fat cell adrenergic receptors and the control of white and brown fat cell function. J Lipid Res. 1993; 34(7):1057–91. [PubMed: 8371057]

[24]. McMahon KK, Schimmel RJ. Apparent absence of alpha-2 adrenergic receptors from hamster brown adipocytes. Life Sci. 1982; 30(14):1185–92. [PubMed: 6283284]

[25]. Elfellah MS, Reid JL. Identification and characterisation of beta-adrenoceptors in guinea-pig skeletal muscle. Eur J Pharmacol. 1987; 139(1):67–72. [PubMed: 2820756]

[26]. Challiss RA, Leighton B, Wilson S, Thurlby PL, Arch JR. An investigation of the beta-adrenoceptor that mediates metabolic responses to the novel agonist BRL28410 in rat soleus muscle. Biochem Pharmacol. 1988; 37(5):947–50. [PubMed: 2830888]

[27]. Roberts SJ, Summers RJ. Cyclic AMP accumulation in rat soleus muscle: stimulation by beta2- but not beta3-adrenoceptors. Eur J Pharmacol. 1998; 348(1):53–60. [PubMed: 9650831]

[28]. Shabalina IG, Backlund EC, Bar-Tana J, Cannon B, Nedergaard J. Within brown-fat cells, UCP1-mediated fatty acid-induced uncoupling is independent of fatty acid metabolism. Biochim Biophys Acta. 2008; 1777(7-8):642–50. [PubMed: 18489899]

[29]. Oana F, Takeda H, Matsuzawa A, Akahane S, Isaji M, Akahane M. Adiponectin receptor 2 expression in liver and insulin resistance in db/db mice given a beta3-adrenoceptor agonist. Eur J Pharmacol. 2005; 518(1):71–6. [PubMed: 15979609]

[30]. Yilmaz Y, Ones T, Purnak T, Ozguven S, Kurt R, Atug O, Turoglu HT, Imeryuz N. Association between the presence of brown adipose tissue and non-alcoholic fatty liver disease in adult humans. Aliment Pharmacol Ther. 2011; 34(3):318–23. [PubMed: 21631560]

[31]. Coman OA, Paunescu H, Ghita I, Coman L, Badararu A, Fulga I. Beta 3 adrenergic receptors: molecular, histological, functional and pharmacological approaches. Rom J Morphol Embryol. 2009; 50(2):169–79. [PubMed: 19434307]

[32]. Baker JG. The selectivity of beta-adrenoceptor antagonists at the human beta1, beta2 and beta3 adrenoceptors. Br J Pharmacol. 2005; 144(3):317–22. [PubMed: 15655528]

[33]. Weyer C, Tataranni PA, Snitker S, Danforth E Jr. Ravussin E. Increase in insulin action and fat oxidation after treatment with CL 316,243, a highly selective beta3-adrenoceptor agonist in humans. Diabetes. 1998; 47(10):1555–61. [PubMed: 9753292]

[34]. Storstein L. Non-receptor-mediated inotropic drugs. Eur Heart J. 1988; 9(Suppl H):91–3. [PubMed: 3049098]

[35]. Arch JR. beta(3)-Adrenoceptor agonists: potential, pitfalls and progress. Eur J Pharmacol. 2002; 440(2-3):99–107. [PubMed: 12007528]

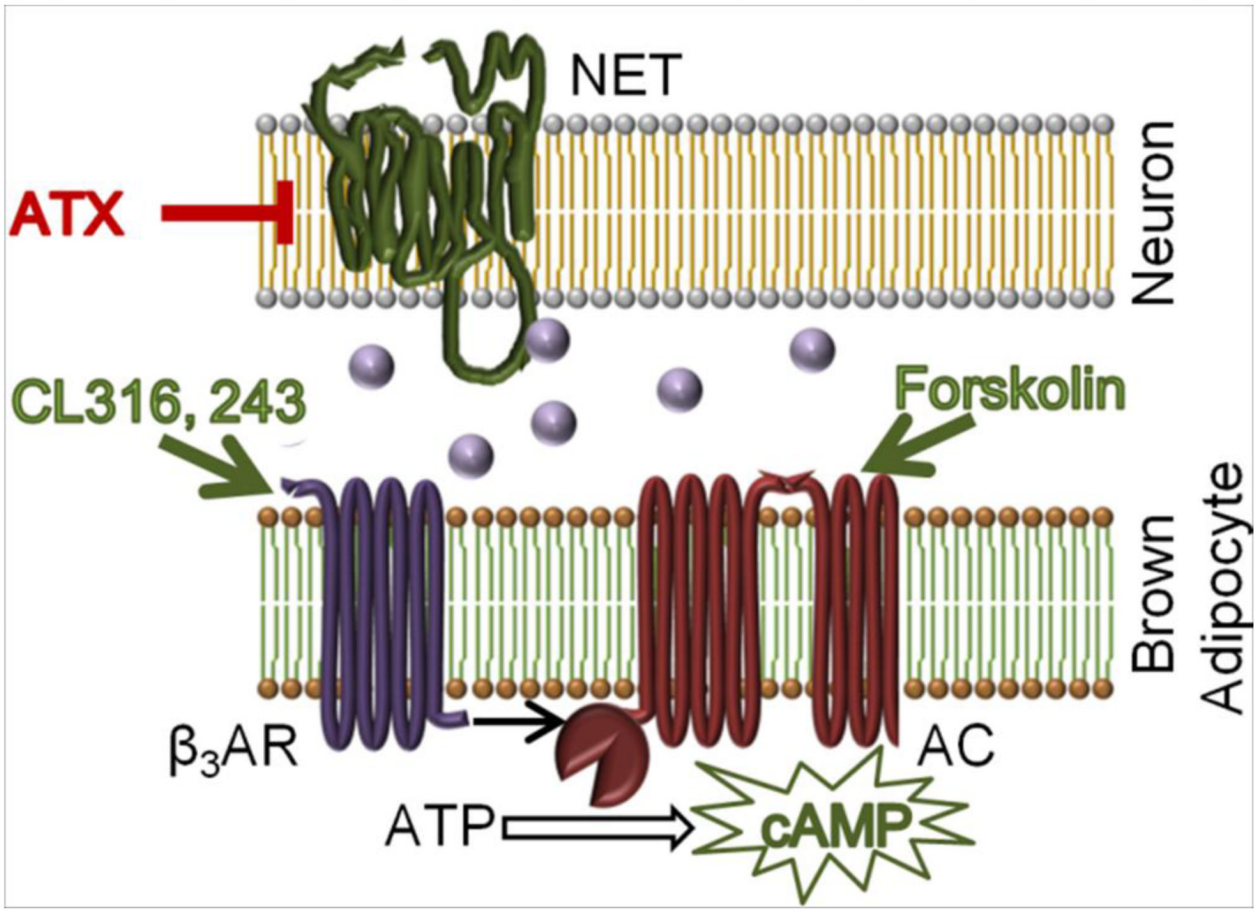

Figure-1.

Schematic showing the synapse of a brown adipocyte. Atomoxetine (ATX) inhibits norepinephrine reuptake by blocking pre-synaptic norepinephrine transporter (NET). CL 316243 (CL) triggers post-synaptic β_3-adrenergic receptor (β_3AR). Forskolin stimulates post-receptor adenylyl cyclase which catalyzes the conversion of ATP to the second messenger cyclic adenosine monophosphate (cAMP). Production of cAMP relays downstream signals which lead to an increase in lipolysis, glycolysis and [^{18}F]FDG uptake.

● Norepinephrine

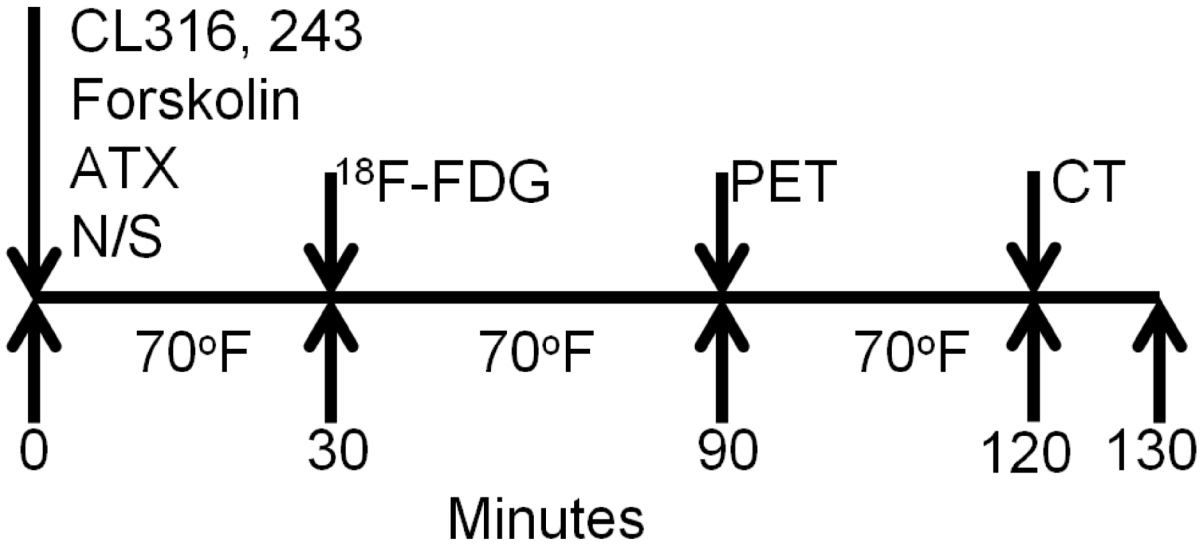

Figure-2.

Study protocol: All mice (n=3, each group) were kept awake in room temperature for additional 60 min prior to 30 minutes PET acquisition followed by 10 minutes CT acquisition for attenuation correction and anatomical delineation of PET images. Fasted mice were injected with either CL 316243 (CL) or Forskolin or atomoxetine (ATX) or normal saline (N/S) 30 minutes prior to [^{18}F]FDG administration.

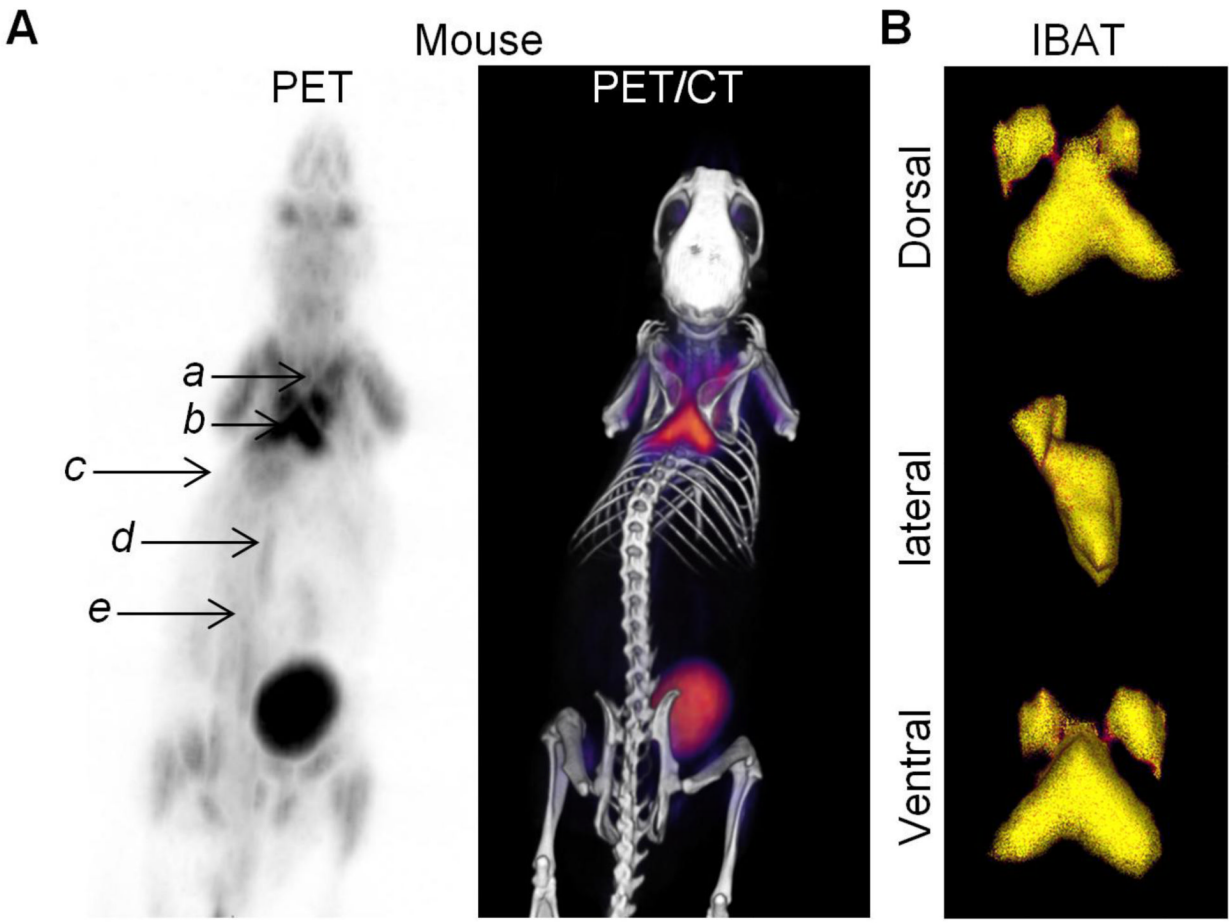

Figure-3.
BAT anatomy in mice: A: 3-D analysis of PET (right) and PET/CT (left) images clearly showing (*a*) cervical, (*b*) interscapular, (*c*) intercostals, (d) periaortic, and (*e*) perirenal BATs in rat. B: 3-D PET images of IBAT in mice: ventral, lateral, and dorsal views.

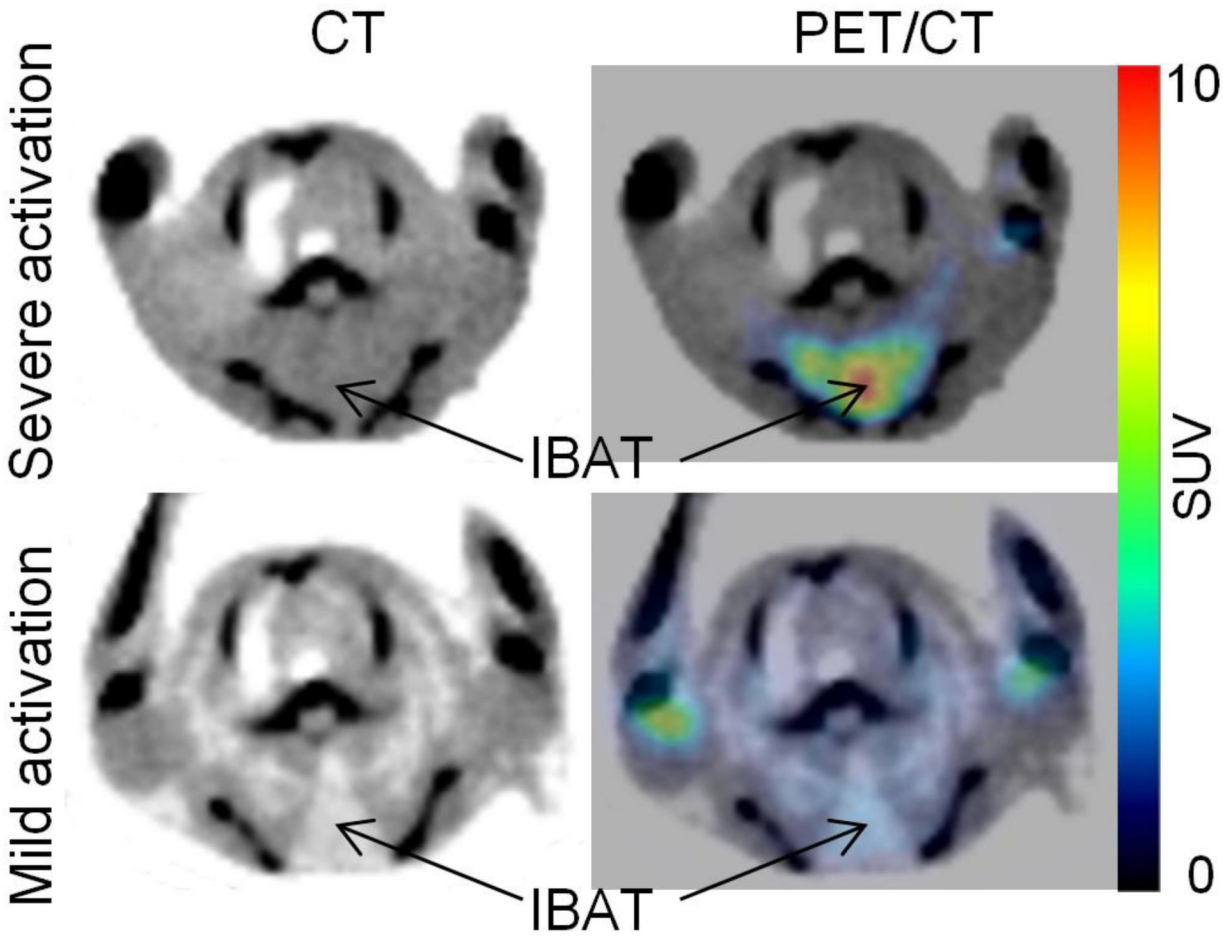

Figure-4.

Transverse views of CT and PET/CT inverse images show high CT HU (dark area) when IBAT [^{18}F]FDG uptake is intense and, low CT HU (light area) when IBAT [^{18}F]FDG uptake is in the same mouse. CT (left) and fused PET/CT (right).

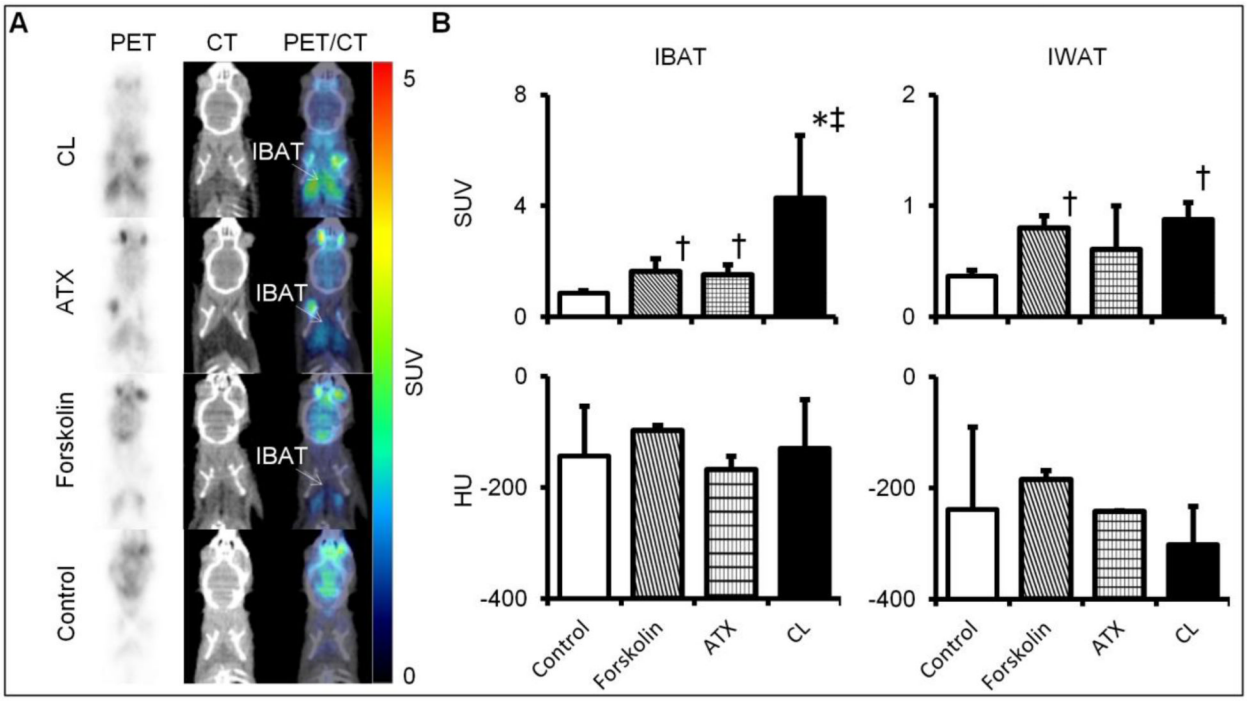

Figure- 5.

Drug effects on mice [^{18}F]FDG PET/CT images A**:** Coronal views of PET/CT images in mice show intense [^{18}F]FDG uptake in the activated IBAT, but faint uptakes in the control group: PET (left), CT (middle) and fused PET/CT (right). B: Quantitative analysis of PET (SUV) and CT (HU) images of IBAT and IWAT in mice treated with drugs compared to control. Data are Mean±SD; *p<0.001, †p<0.05 compared with control; ‡p<0.01 compared with ATX and forskolin (n=3, each group).

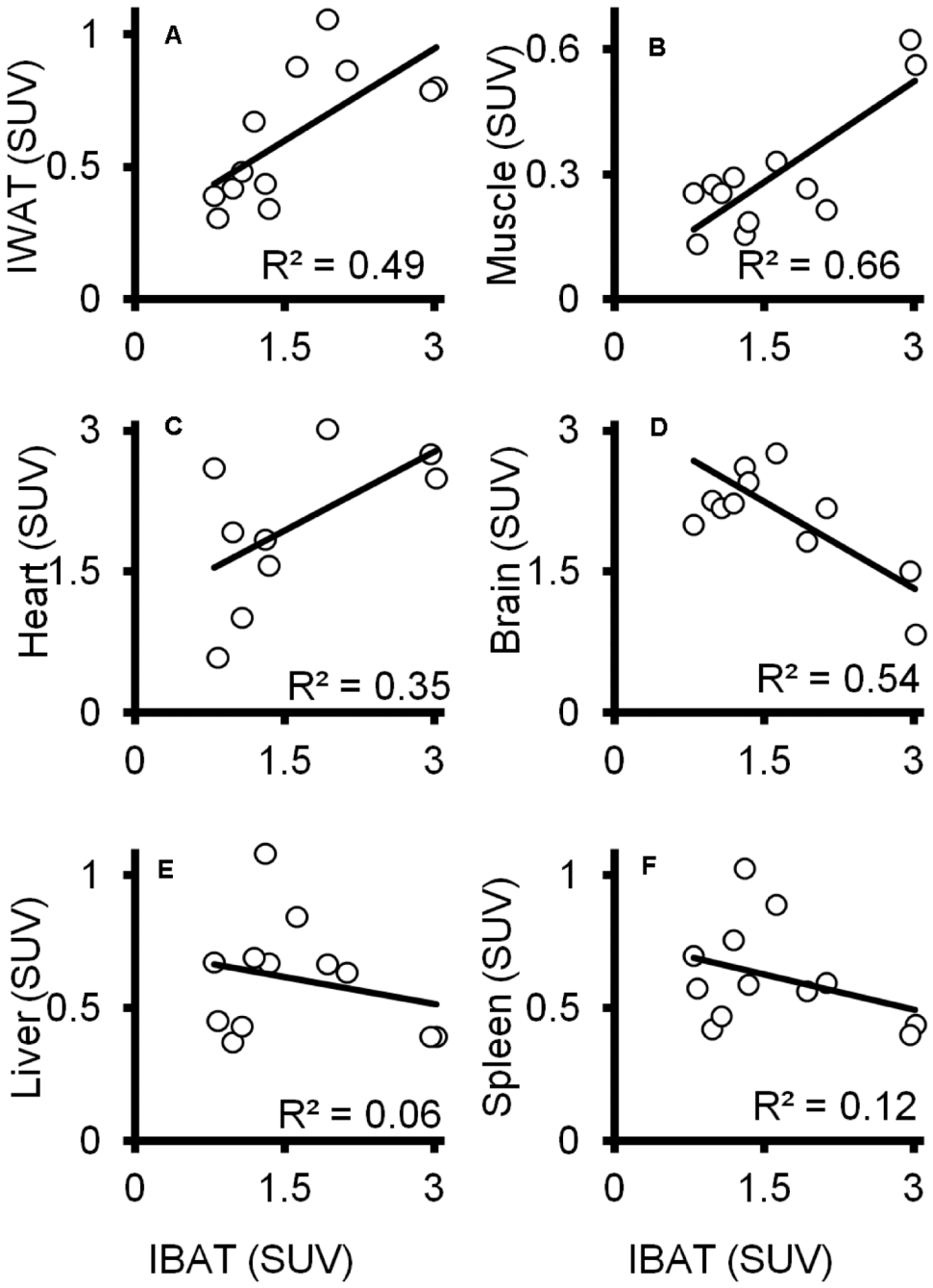

Figure- 6.
Bivariate analysis of IBAT [^{18}F]FDG SUV versus those of IWAT, muscle, brain, heart, liver, and spleen.

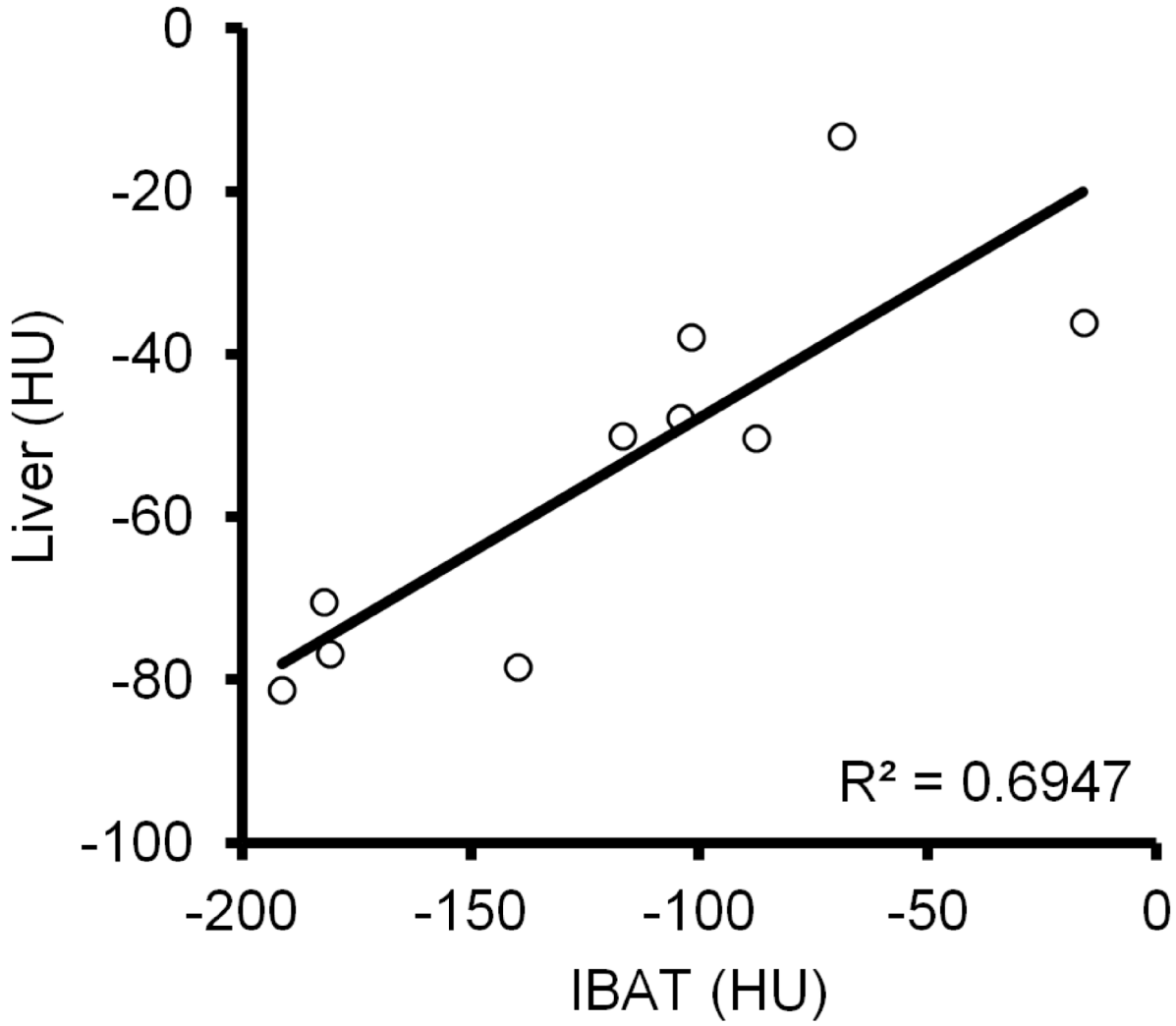

Figure-7.
Bivariate analysis of IBAT [^{18}F]FDG SUV versus CT HU. A: SUV: 0-3 and B: SUV: 0-10.

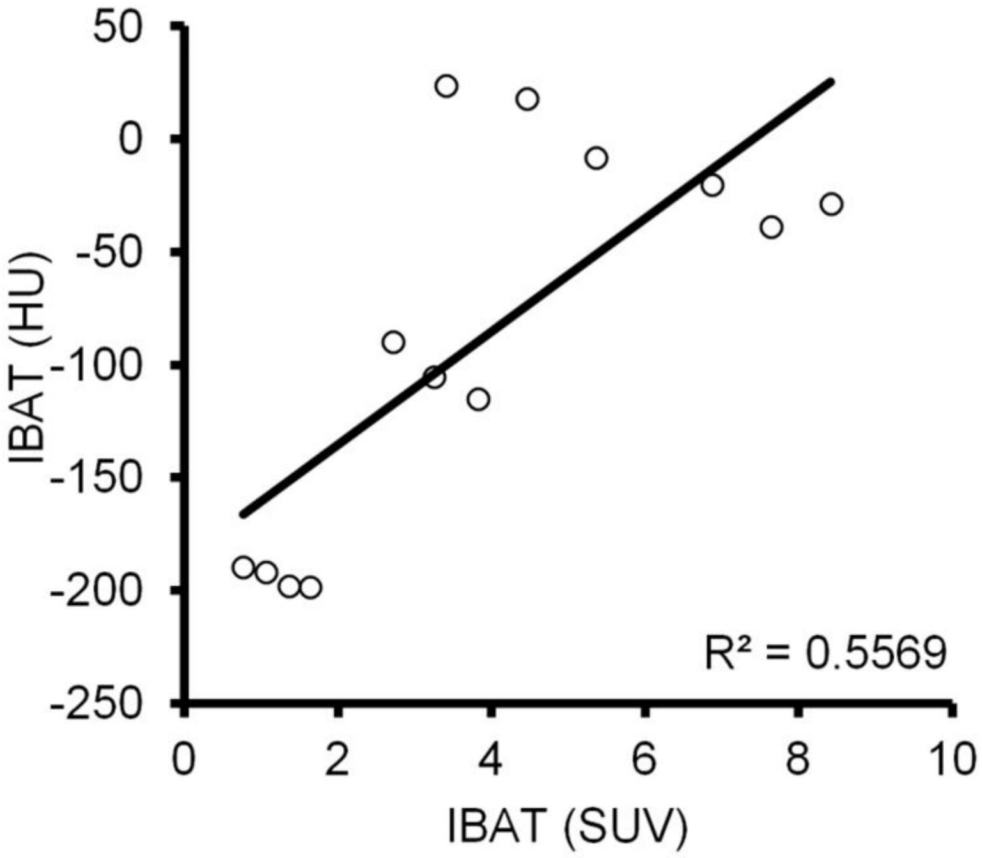

Figure-8.
Bivariate analysis of IBAT CT HU versus Liver CT HU.

Table 1

Quantitative analysis of PET (SUV) images of all regions of interest

ROIs [a]	Control	Forskolin	ATX	CL316, 243	*p* value [b]
IBAT	0.86±0.09	1.64±0.47 [e]	1.52±0.35 [e]	4.28±2.25 [fg]	0.002
IWAT	0.37±0.06	0.80±0.12 [e]	0.61±0.39	0.88±0.15 [e]	0.042
Heart [c]	1.18±1.0	6.42±2.77 [h]	2.15±0.77	2.70±0.18	0.043
Muscle [d]	0.22±0.07	0.28±0.06	0.20±0.06	0.59±0.03 [f]	0.001
Brain	2.55±0.73	2.39±0.32	2.30±0.41	1.54±0.72	0.226
Spleen	0.56±0.14	0.74±0.14	0.73±0.26	0.45±0.06	0.182
Liver	0.49±0.15	0.72±0.11	0.80±0.24 [h]	0.38±0.02	0.012

n=3 in each group. Data are Mean±SD

Obtained by post hoc LSD test:

[a] Regions of interest

[b] Obtained by ANOVA test

[c] Cardiac muscle

[d] Skeletal muscle (Triceps)

[e] $p<0.05$

[f] $p<0.001$ compared with control

[g] $p<0.01$ compared with ATX and forskolin

[h] $p<0.01$ compared with control